COMPUTATIONAL MODELLING OF DUMP COMBUSTORS FLOWFIELD

D. Lentini
Dipartimento di Meccanica e Aeronautica
Universita' degli Studi di Roma "La Sapienza"
00184 Rome, Italy

W.P. Jones
Department of Chemical Engineering and Chemical Technology
Imperial College of Science, Technology and Medicine
London SW7 2BY, United Kingdom

ABSTRACT

A computational model aimed at predicting the flowfield of dump combustors is presented. The turbulent combustion model is based on the conserved scalar approach and on a convenient specification of its probability density function, which reduces the computation of the mean density to a closed form. Turbulence is modelled by means of the k-ϵ model. The averaged conservation equations are solved by a technique based on a staggered grid and on the SIMPLE solver.

The computational model is applied to a simple dump combustor to assess the computer time requirements and accuracy. The turbulent combustion model here introduced is shown to reduce the computer time by an order of magnitude when compared to evaluating the mean density by numerical quadrature.

NOMENCLATURE

a,b	exponents of the beta-function
c_j	coefficients of polynomial approximation of F(f)
C	normalization constant of the beta function
C_{g1}, C_{g2}	constants in the equation for the variance of the conserved scalar
$C_{\epsilon 1}$, $C_{\epsilon 2}$	constants in the equation for the viscous dissipation rate
C_μ	constant in the expression for the turbulent viscosity
f	conserved scalar
F(f)	quantity defined by eq. (4)
k	turbulent kinetic energy
$h_k(\tilde{f},\tilde{f''^2})$	factor defined by eq. (14)
$H(\tilde{f},\tilde{f''^2})$	function defined by eq. (13)
I_j	integral defined by eq. (11)
J	order of the polynomial approximation of F(f)
p	pressure
$\bar{p}^*$	quantity defined by eq. (2)
P(f)	probability density function of the conserved scalar

P_g, P_k	production terms defined by eqs. (3)
r	radial coordinate
R^0	universal gas constant
T	temperature
u, v	velocity components in x and r
$\tilde{W}$	mixture mean molecular weight
x	axial coordinate
ϵ	viscous dissipation rate
Φ	generic quantity
μ	molecular viscosity
μ_t	turbulent viscosity
ρ	density
ρ_{ref}	reference density
σ	molecular Prandtl number
σ_f, σ_g, σ_k, σ_ϵ	effective turbulent Prandtl numbers

Subscripts

$(\ )_r$	derivative with respect to r
$(\ )_x$	derivative with respect to x

Superscripts

$(\bar{\ })$	conventional average
$(\tilde{\ })$	Favre average
$(\ )'$	fluctuation about conventional average
$(\ )''$	fluctuation about Favre average

1. INTRODUCTION

Flameholding in subsonic combustion ramjets is achieved by using dump combustors, in which the flame is anchored to the chamber by a large region of recirculation. The ensuing elliptic character of the flow imposes however a considerable stress on the numerical simulation of such flowfields. Special grid arrangements and computational techniques must therefore be used, and the computational requirements are demanding. The problem is compounded with that of providing an adequate representation of the effects of turbulent fluctuations on combustion. For nonpremixed flames the most popular approach is that making use of a presumed probability density function (pdf) of a conserved scalar quantity (ref. 1). The effect of turbulent fluctuations is thus restricted to the mean density $\bar{\rho}$, which is computed via an appropriate integral. The accurate evaluation of such integrals, which must be computed at each node point and at each computational step, requires a large number of intervals and takes therefore the largest share of the overall computing time.

Three examples of previous applications of computer codes to the solution of dump combustor flowfields in subsonic combustion ramjets are worthy of note. Harsha et al. (ref. 2) reduced the computer time to an acceptable level (4 to 15 minutes on a CDC 7600)

by separating the computation of the directed flow from that of the recirculation region: this requires an a priori knowledge of the reattachment length, so that this code cannot be considered to be a truly predictive tool. Further, no account was taken of the effect of fluctuations on combustion. Drummond (ref. 3) performed a unified calculation of the combustor flowfield, but the computer time was exceedingly high, even for nonreacting computations, in which 150000 steps and 4.6 hours on a CYBER 203 were needed. When reacting flowfields were considered the number of iterations rose to 200000, and the convergence of the solution was poor; the computer time is not reported. Also the combustion model did not account for the effects of fluctuations. The difficulty in obtaining a converged solution might be ascribed to the grid arrangement and the algebraic eddy viscosity model used, which appears not be suited to recirculating flows. A sounder computational model was presented by Vanka et al. (ref. 4) for ducted rockets, a ramjet variant. They correctly account for the effects of fluctuations by specifying the conserved scalar pdf as a battlement shaped function. The inherently three-dimensional character of the flowfield in this case requires using a rather coarse mesh ($24 \times 11 \times 11$) to limit the computing time to 25 minutes on an IBM 3033.

The intent of the present paper is to show that, by introducing suitable assumptions to effect the thermochemical closure of the model, a very large reduction in computer time can be achieved. This is substantiated by applying the present model to a simple hydrogen-air dump combustor. In the following Section the describing equations are introduced, and then in Sec. 3 the proposed model for the thermochemical closure of such equations is presented.

2. CONSERVATION EQUATIONS

The bases of the analysis of the flowfield of nonpremixed turbulent combustion are the averaged conservation equations for mass, momentum and a scalar quantity f. The latter represents either a normalized enthalpy or atomic mass fraction: in fact, with the assumption that the kinetic energy is neglegible in the energy equation (implying relatively low-speed flow), that the diffusion can be represented in terms of a single coefficient, and that the Lewis number is unity, the equations for the above mentioned scalar quantities assume the same form, free of source terms. Favre-averaging (see e.g. ref. 5) is used to account for the effects of variable density: for a generic quantity Φ, it gives

$$\tilde{\Phi} = \frac{\overline{\rho\Phi}}{\bar{\rho}} \qquad\qquad \Phi'' = \Phi - \tilde{\Phi}$$

where the tilde denotes the Favre mean, the overbar a conventional average, and the double prime the fluctuation about the Favre mean. Conventional averages are retained for the mean pressure $\bar{p}$ and density $\bar{\rho}$. Turbulence is modeled according to the k-ϵ model, which is generally accepted as the most reliable compromise between rather crude algebraic eddy viscosity models and second-order closure models. The latter are rather complicated and still not fully tested (see ref. 6, although considerable progress has been recently reported by Jones and Pascau, ref. 7). To complete the model equations for the mean $\tilde{f}$ and the variance $\widetilde{f''^2}$ of the conserved scalar (ref. 1) are included in the formalism. Molecular diffusion terms are retained for completeness to account for near-wall and possible low Reynolds number effects (ref. 8), in particular at the inlet. As they are relatively important only in regions where the intensity of the fluctuations is low, such fluctuations are neglected in their evaluation. The steady, axisymmetric form of the conservation equations is considered.

Thus, the averaged equations for mass, axial and normal momentum, turbulent kinetic energy $\tilde{k}$, viscous dissipation rate $\tilde{\epsilon}$, and for the mean and the variance of the conserved scalar are

$$\left(\bar{\rho}\tilde{u}\right)_x + \frac{1}{r}\left(r\bar{\rho}\tilde{v}\right)_r = 0 \tag{1a}$$

$$\bar{\rho}\tilde{u}\tilde{u}_x + \bar{\rho}\tilde{v}\tilde{u}_r = \left[2\ (\mu + \mu_t)\ \tilde{u}_x\right]_x + \frac{1}{r}\left[r\ (\mu + \mu_t)\ (\tilde{u}_r + \tilde{v}_x)\right]_r - \bar{p}^*_x \tag{1b}$$

$$\bar{\rho}\tilde{u}\tilde{v}_x + \bar{\rho}\tilde{v}\tilde{v}_r = \left[(\mu + \mu_t)\ (\tilde{v}_x + \tilde{u}_r)\right]_x + \frac{1}{r}\left[2r\ (\mu + \mu_t)\ \tilde{v}_r\right]_r - \bar{p}^*_r \tag{1c}$$

$$\bar{\rho}\tilde{u}\tilde{f}_x + \bar{\rho}\tilde{v}\tilde{f}_r = \left[(\frac{\mu}{\sigma} + \frac{\mu_t}{\sigma_f})\ \tilde{f}_x\right]_x + \frac{1}{r}\left[r\ (\frac{\mu}{\sigma} + \frac{\mu_t}{\sigma_f})\ \tilde{f}_r\right]_r \tag{1d}$$

$$\bar{\rho}\tilde{u}\tilde{k}_x + \bar{\rho}\tilde{v}\tilde{k}_r = \left[(\mu + \frac{\mu_t}{\sigma_k})\ \tilde{k}_x\right]_x + \frac{1}{r}\left[r\ (\mu + \frac{\mu_t}{\sigma_k})\ \tilde{k}_r\right]_r + P_k - \bar{\rho}\tilde{\epsilon} \tag{1e}$$

$$\bar{\rho}\tilde{u}\tilde{\epsilon}_x + \bar{\rho}\tilde{v}\tilde{\epsilon}_r = \left[(\mu + \frac{\mu_t}{\sigma_\epsilon})\ \tilde{\epsilon}_x\right]_x + \frac{1}{r}\left[r\ (\mu + \frac{\mu_t}{\sigma_\epsilon})\ \tilde{\epsilon}_r\right]_r + C_{\epsilon 1}\frac{\tilde{\epsilon}}{\tilde{k}}P_k - C_{\epsilon 2}\frac{\bar{\rho}\tilde{\epsilon}^2}{\tilde{k}} \tag{1f}$$

$$\bar{\rho}\tilde{u}\tilde{f''^2}_x + \bar{\rho}\tilde{v}\tilde{f''^2}_r = \left[(\frac{\mu}{\sigma} + \frac{\mu_t}{\sigma_g})\ \tilde{f''^2}_x\right]_x + \frac{1}{r}\left[r\ (\frac{\mu}{\sigma} + \frac{\mu_t}{\sigma_g})\ \tilde{f''^2}_r\right]_r + C_{g1}P_g - C_{g2}\frac{\bar{\rho}\tilde{\epsilon}\tilde{f''^2}}{\tilde{k}} \tag{1g}$$

$\bar{p}^*$ is defined as

$$\bar{p}^* = \bar{p} - \frac{2}{3}\left\{(\mu + \mu_t)\ [\tilde{u}_x + \frac{1}{r}\ (r\ \tilde{v})_r] + \bar{\rho}\ \tilde{k}\right\} \tag{2}$$

and the production rates are given by

$$P_k = \mu_t\left[\ \tilde{v}_x^{\,2} + \tilde{u}_r^{\,2} + 2\left(\tilde{u}_x^{\,2} + \tilde{v}_r^{\,2} + \tilde{v}_x\ \tilde{u}_r\right)\right] \tag{3a}$$

$$P_g = \mu_t\left(\ \tilde{f}_x^{\,2} + \tilde{f}_r^{\,2}\ \right) \tag{3b}$$

The turbulent viscosity is given as

$$\mu_t = C_\mu\ \bar{\rho}\ \frac{\tilde{k}^2}{\tilde{\epsilon}}$$

σ has the meaning of a molecular Prandtl number. The model constants are taken as (refs. 9 and 6)

$\sigma_f = 0.7$ $\quad \sigma_k = 1$ $\quad \sigma_\epsilon = 1.3$ $\quad \sigma_g = \sigma_f$

$C_{\epsilon 1} = 1.44$ $\quad C_{\epsilon 2} = 1.92$ $\quad C_{g1} = \frac{2}{\sigma_f}$ $\quad C_{g2} = 2$

$C_\mu = 0.09$

Eqs. (1) represent a set of seven differential equations for the variables $\tilde{u}$, $\tilde{v}$, $\bar{p}^*$, $\tilde{f}$, $\tilde{k}$, $\tilde{\epsilon}$, $\tilde{f''^2}$.

In order to close this set, the mean density $\bar{\rho}$ must be expressed as a function of the state variables considered.

3. THERMOCHEMICAL CLOSURE

Following the conserved scalar approach, all state quantities can be determined as a function of a single scalar quantity f, which is taken here as the elemental mass fraction of hydrogen. In fact, with the assumption that the pressure is thermochemically constant, the mixture composition and temperature (as well as any further state variable) are determined by chemical equilibrium computations, as a function of f alone. Thus from the equation of state:

$$\rho = \frac{p}{\frac{R^0}{\bar{W}} T}$$

where R^0 is the universal gas constant and $\bar{W}$ is the mixture average molecular weight, the density too turns out to be a function of f alone. The above equation can be rewritten for convenience as

$$\rho = \frac{\rho_{ref}}{F(f)} \tag{4}$$

where F(f) is a function of f determined by equilibrium computations; ρ_{ref} is a reference density, introduced to make this function dimensionless.

In order to evaluate the mean density, a probability density function (pdf) for the conserved scalar must be introduced, such that P(f) df is the fraction of time the conserved scalar is bounded between the values f and f+df. The mean density is then obtained from:

$$\bar{\rho} = \rho_{ref} \int_0^1 \frac{P(f)}{F(f)} \, df \tag{5}$$

The pdf shape is assigned a priori, since it can be shown (ref. 1) that the result is relatively insensitive to the specific pdf assumed. Its parameters are determined on the basis of the mean $\tilde{f}$ and the variance $\tilde{f''^2}$ of the conserved scalar, for which appropriately modelled differential equations are solved. In the present model (refs. 10, 11), developed after a suggestion by Libby (ref. 12), F(f) is approximated by a J-th order polynomial fit

$$F(f) \cong \sum_{j=0}^{J} c_j \, f^j \tag{6}$$

and a pdf is specified for the whole ratio P(f)/F(f) as a beta-function

$$\frac{P(f)}{F(f)} = C \, f^{a-1}(1-f)^{b-1} \tag{7}$$

where C is a normalization constant and the exponents a and b of the beta-function are related to the mean and the intensity of the conserved scalar through the expressions (ref. 13)

$$a = \frac{\tilde{f}^2\,(1-\tilde{f})}{\widetilde{f''^2}} - \tilde{f}$$

$$b = \frac{\tilde{f}\,(1-\tilde{f})^2}{\widetilde{f''^2}} - (1-\tilde{f}) \qquad (8)$$

Intermittency at the edges of the mixing layer is not accounted for explicitly in the present model. In any case, the beta-function itself accounts for intermittency to some extent, by giving a finite probability to the states $f = 0$ (if $a < 1$) and $f = 1$ (if $b < 1$).

To determine the parameter C, the normalization condition

$$\int_0^1 P(f)\,df = 1$$

is enforced. Its left-hand side can be written as

$$C \int_0^1 f^{a-1}(1-f)^{b-1}F(f)df \cong C \sum_{j=0}^{J} c_j I_j(a,b) \qquad (10)$$

where use has been made of approximation (6); the integrals I_j (j=0,1,...,J), defined as

$$I_j(a,b) = \int_0^1 f^{a-1+j}(1-f)^{b-1}df \qquad (11)$$

are expressed through the relation (derived after ref. 14)

$$I_j(a,b) = \frac{\Gamma(a+j)\Gamma(b)}{\Gamma(a+b+j)}$$

Thanks to properties of the gamma-function, the summation appearing in (10) can be expressed as

$$\sum_{j=0}^{J} c_j I_j(a,b) = I_0(a,b) \sum_{j=0}^{J} c_j \prod_{k=1}^{j} \frac{a+k-1}{a+b+k-1}$$

This allows C to be determined. Upon substitution in (7) and then in (5), the mean density is obtained as

$$\bar{\rho} = \frac{\rho_{ref}}{H(\tilde{f},\widetilde{f''^2})} \qquad (12)$$

with

$$H(\tilde{f},\widetilde{f''^2}) = \sum_{j=0}^{J} c_j \prod_{k=1}^{j} h_k(\tilde{f},\widetilde{f''^2}) \qquad (13)$$

and (k = 1,2,...,J)

$$h_k(\tilde{f},\widetilde{f''^2}) = \qquad (14)$$

$$= \tilde{f} + \frac{(k-1)\,(1-\tilde{f})}{k - 2 + \dfrac{\tilde{f}\,(1-\tilde{f})}{\widetilde{f''^2}}} \qquad \text{for } 0 < \tilde{f} < 1$$

$$= \tilde{f} \qquad \text{for } \tilde{f} = 0,\ 1$$

where use has been made of (8).

This formulation has the advantage of reducing the integral appearing in (5) to a closed form. Further, the probability density function here introduced has been shown to give results fully consistent with experimental data (ref. 11).

4. NUMERICAL ALGORITHM

The present model for the mean density $\tilde{\rho}$ has been introduced into the computer program JETFLO (ref. 15). This code is based on use of a staggered grid (ref. 16) and SIMPLE solver. The converged solution is obtained by iteration. Synthetic wall boundary conditions are enforced to avoid resolving the boundary layer, which would otherwise take the largest share of computing time.

F(f) is approximated by a 12th order polynomial fit. The equilibrium conditions for the hydrogen-air flow considered here are computed by means of the equilibrium chemistry program STANJAN (ref. 17); the included species are Ar, H, H_2, H_2O, N, N_2, NO, NO_2, O, O_2, OH.

5. TEST CASE

The present model is here applied to a simple cylindrical dump combustor. The main aim of this test case is to quantify the reduction of computing time achieved with the present turbulent combustion model, rather than to present an accurate computation of a practical combustor. Some limitations of the configuration being considered (i.e., the quite low Mach number and equivalence ratio) and of the computational implementations (i.e., the rather coarse mesh and the approximate specification of the inlet conditions) must be viewed in this perspective; they are introduced only for the sake of computational convenience and to limit the CPU time to an amount convenient for initial testing. The test case is computed with four different options, labelled 1 to 4:

1) 28 × 28 grid, $\tilde{\rho}$ given by the present model
2) 15 × 15 grid, $\tilde{\rho}$ given by the present model
3) 15 × 15 grid, $\tilde{\rho}$ computed by numerical quadrature over 200 intervals
4) 15 × 15 grid, $\tilde{\rho}$ computed by numerical quadrature over 100 intervals

In runs 3 and 4 the probability density function P(f) of the conserved scalar is taken as a beta-function.

The results of run 1 are presented in detail as the most accurate ones. A comparison of the results of runs 1 and 2 is used to give some indications as to what an extent the solution may be considered grid independent. The comparison of CPU time of runs 2 and 3 is used to quantify the reduction achieved by the present model, as compared to evaluating $\tilde{\rho}$ by numerical quadrature over 200 intervals. In order to assess whether 200 intervals are adequate for estimating $\tilde{\rho}$, a comparison of the results of runs 3 and 4 is used.

The dump combustor considered in this test case is fed with hydrogen, injected through the central pipe (0.0077 m internal radius, 0.0154 m outer radius) at 1 m/s, and air, supplied through a 0.0115 m wide annulus at 10 m/s. The combustor internal radius is 0.05 m, resulting in a rearward facing step 0.0231 m high at the inlet; its length is 0.3 m. The velocity profiles at the inlet are assumed to be flat for each stream for simplicity. In any event this oversimplified assumption is unlikely to affect the overall

flowfield to a significant extent in elliptic flows and, moreover, the definition of the initial conditions for the test case being considered involves much larger incertainties, as will be apparent in the following paragraph.

Figure 1 reports the main features of the combustor flowfield, as computed in run 1. In particular, Fig. 1a reports stream function isolines, i.e., streamlines. A recirculation zone appears downstream of the dump plane and ensures flame stabilization. Due to the very low density of hydrogen, as well as to its low inlet velocity in this test case, such isolines are widely separated near the centerline, thus giving a rather poor representation of the flowfield. It is possible however to identify a smaller region of local recirculation near the hydrogen inlet, due to its inlet velocity being substantially lower than the other stream. It appears likely that such a recirculation spot reaches into the hydrogen supply pipe, thus invalidating the assumption of fully developed flow used at the inlet for computational purposes. This should however only affect the flowfield in the immediate neighbourhood of the hydrogen inlet, and have limited effects on the overall flow pattern. However this does suggest that a specification of the initial velocity profiles more accurate than that hypothesized above is unwarranted, at least in this case. The solution would be to extend the computational domain upstream into the hydrogen supply pipe. In Fig. 1b the isolines of the logarithm of the mean value of the conserved scalar are shown. A rapid mixing is observed close to the plate separating the hydrogen and air streams. The stoichiometric combustion of hydrogen and air corresponds to $f = 0.0284$, so that the isoline -1.5 is very close to the mean location of the stoichiometric contour, albeit somewhat on the rich side. Of course, due to the fluctuations, such a front is highly oscillating. An estimate of the intensity of such oscillations can be obtained from Fig. 1c which shows the isolines of the logarithm of the variance of the conserved scalar. The intensity of the fluctuations appears to be maximum close to the flame front.

Figure 2 displays (for run 1) the isolines of the mean and the intensity of state quantities which are recovered from the mean and the variance of the conserved scalar via its assumed probability density function. For the mean density $\bar{\rho}$, the form (12) is used. For any other state quantity (but the pressure) Φ, both conventional and Favre averages can be recovered as

$$\bar{\Phi} = \int_0^1 \Phi(f)\ P(f)\ df$$

$$\tilde{\Phi} = \frac{\overline{\rho\Phi}}{\bar{\rho}} = \frac{1}{\bar{\rho}} \int_0^1 \rho(f)\ \Phi(f)\ P(f)\ df$$

Further, the intensity of the fluctuations can be obtained as

$$\overline{\Phi'^2} = \int_0^1 [\Phi(f)-\bar{\Phi}]^2\ P(f)\ df$$

and similarly for $\tilde{\Phi}''^2$.

In these expressions, $\Phi(f)$ denotes the equilibrium value of Φ as a function of the conserved scalar. The evaluation of such integrals was achieved by numerical quadrature. However the contribution to the overall computing time is negligible as they need only be computed at the last iteration. The computation is further expedited by limiting the integration range to the domain

$$[\max(\ 0,\ \tilde{f}-6\sqrt{\tilde{f''^2}}),\ \min(\ 1,\ \tilde{f}+6\sqrt{\tilde{f''^2}})]$$

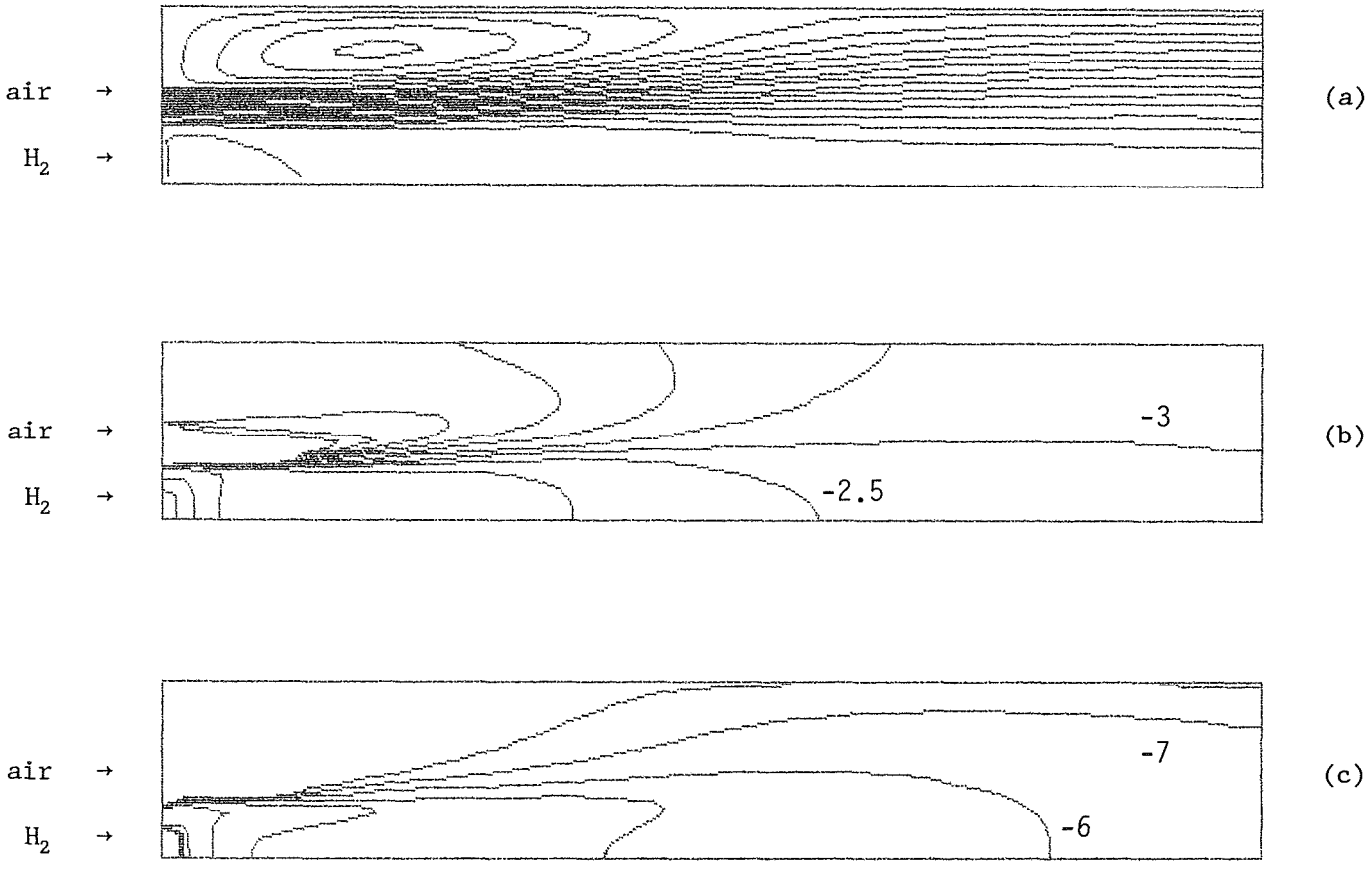

Fig. 1. Isoline plots: a) stream function (streamlines), b) logarithm of the mean of the conserved scalar, c) logarithm of the variance of the conserved scalar.

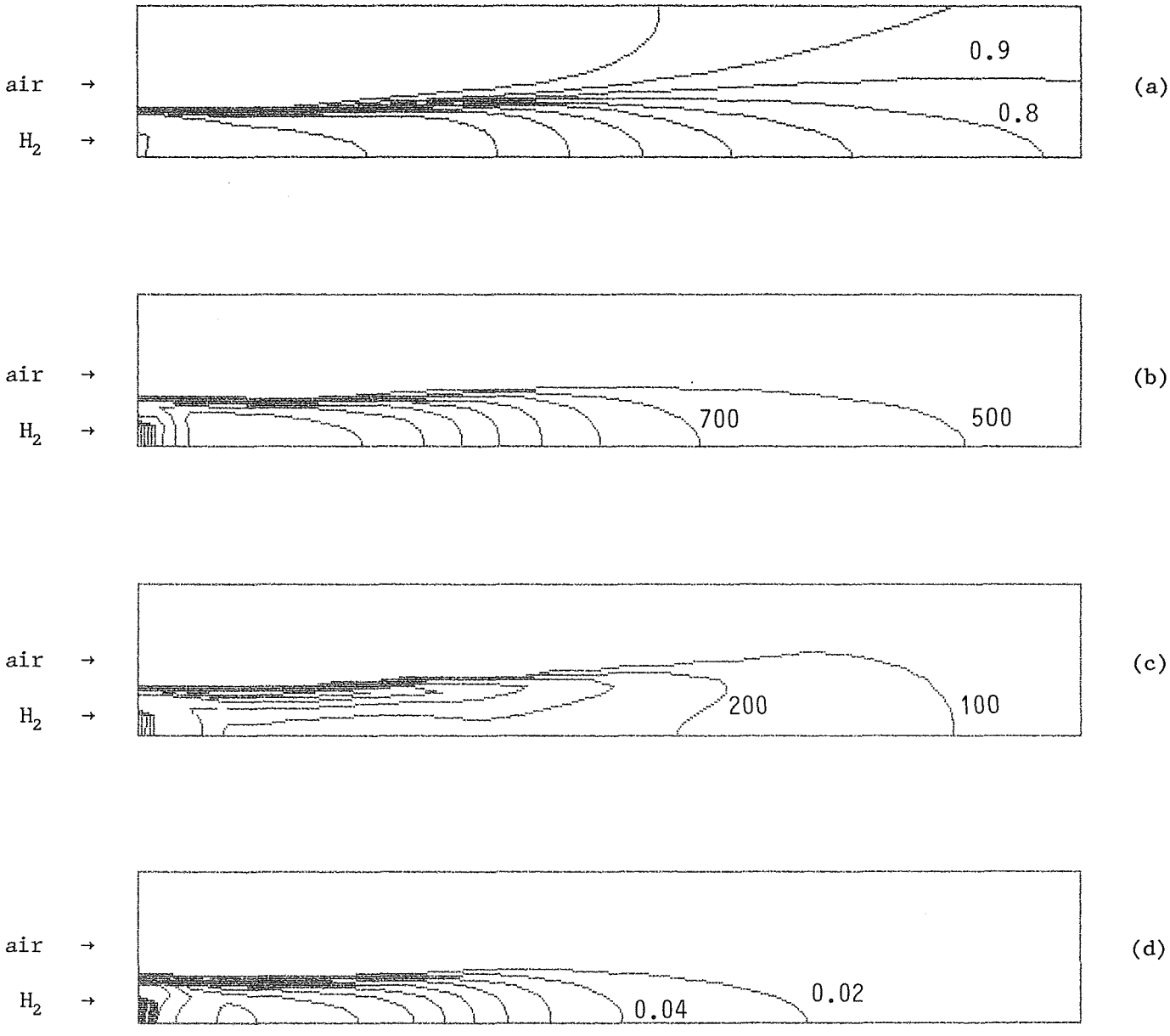

Fig. 2. Isoline plots: a) mean density (kg/m^3), b) mean temperature ($^\circ$K), c) rms of temperature fluctuations ($^\circ$K), d) mean water vapour mass fraction.

rather than [0,1].

Figures 2a through 2d show isolines of the average density, average temperature, rms of temperature fluctuations and average water vapour mass fraction, respectively. Conventional averages are reported for temperature as measurements by thermocouples give unweighted means, whereas Favre-averaging is used for the mass fraction as probe sampling results in close to density-weighted concentrations. It can be seen that the temperature at the exit of the combustor is rather low due to the large excess air involved in this particular test case. Mean temperatures about 2100 °K are predicted near the flame zone, with accompanying rms of fluctuations in excess of 770 °K. The mean water vapour mass fraction at the exit is rather low as well.

We will now briefly compare the results of the different runs in terms of accuracy and CPU time.

By comparing runs 1 and 2, it can be seen that the mean axial velocity component computed with the coaser grid (step size doubled in both directions) exhibits a maximum difference of 25% of the maximum velocity with respect to that computed with the finer grid. Although this may not represent a sufficiently grid-converged solution for most purposes, it is believed that the 28 × 28 grid gives results at least indicative of the overall flowfield configuration. Run 1 requires 443 iterations and 50.16 s CPU time on an IBM 3090/600 processor; the computation is assumed to be converged when the residuals of all quantities are less than 10^{-4}.

The comparison of the CPU time requirements of the present model ($\tilde{\rho}$ in closed form) and of a more conventional approach ($\tilde{\rho}$ evaluated by numerical quadrature) is performed on a 15 × 15 points grid, because the latter model involves very long computer runs. By comparing runs 2 (196 iterations and 6.11 s CPU time) and 3 (375 iterations and 62.22 s), it can be seen that the present model cuts the CPU time by a factor ten when compared to a numerical quadrature over 200 intervals.

The question remain to be addressed whether 200 intervals are enough to ensure an accurate evaluation of $\tilde{\rho}$. To this ends, the results of run 3 can be compared to those of run 4 (numerical quadrature over 100 intervals). The relative difference between the values of $\tilde{\rho}$ computed with the two runs reaches a maximum of about 4%. This seems to indicate that the 200 intervals considered in run 3 might be adequate for a reasonably accurate computation, but 100 intervals might not.

6. CONCLUSIONS

The present model defines a soundly based treatment for nonpremixed turbulent combustion and, thanks to an appropriate assumption for the conserved scalar pdf, reduces the computer time requirements by about an order of magnitude in elliptic flows.

REFERENCES

1. Bilger, R.W., "Turbulent flows with nonpremixed reactants", in *Turbulent reacting flows* (eds. P.A. Libby and F.A. Williams), Topics in applied physics 44, 65-113, Springer-Verlag, Berlin (1980).

2. Harsha, P.T., Edelman, R.B., Schmotolocha, S.N. and Pederson, R.J., "Combustor modeling for ramjet development programs", in *AGARD CP 307* (1981).

3. Drummond, J.P., "Numerical study of a ramjet dump combustor flowfield", *AIAA J.*, 23, 604-611 (1985).

4. Vanka, S.P., Craig, R.R. and Stull, F.D., "Mixing, chemical reaction and flowfield development in ducted rockets", *J. Prop. P.*, 2, 331-338 (1986).

5. Libby, P.A. and Williams, F.A., "Fundamental aspects", in *Turbulent reacting flows* (eds. P.A. Libby and F.A. Williams), Topics in applied physics 44, 1-43, Springer-Verlag, Berlin (1980).

6. Jones, W.P. and Whitelaw, J.H., "Calculation methods for turbulent reacting flows: a review", *Comb. Flame*, 48, 1-26 (1982).

7. Jones, W.P. and Pascau, A., "Calculation of confined swirling flows with a second moment closure", *J. Fluids Engineering, Trans. ASME*, 111, 248-255 (1989).

8. Patel, V.C., Rodi, W. and Scheurer, G., "Turbulence model for near-wall and low Reynolds number flows: a review", *AIAA J.*, 23, 1308-1319 (1985).

9. Rodi, W., *Turbulence models and their application to hydraulics - a state of the art review.* Int. Ass. Hydraulic Research, Delft (1980).

10. Lentini, D., "Modelling and simulation of nonpremixed turbulent flames", *IV Conv. It. Mecc. Comp.*, Padova (1989). Also submitted to *Meccanica.*

11. Lentini, D., "Numerical prediction of nonpremixed turbulent flames", AIAA paper 90-0730 (1990).

12. Libby, P.A., Private communication (1988).

13. Jones, W.P., "Models for turbulent flows with variable density and combustion", in *Prediction models for turbulent flows*, (ed. W. Kollmann), 380-421, Hemisphere Publ. Co., Washington (1980).

14. Abramowitz, M. and Stegun, I.A., *Handbook of mathematical functions*, National Bureau of Standards, Washington (1964).

15. Jones, W.P. and McGuirk, J.J., "Computational fluid dynamics of turbulent flows", Short course lecture notes, Univ. Zaragoza (1984).

16. Harlow, F.H. and Welch, J.E., "Numerical calculation of time-dependent viscous incompressible flow of fluids with free surface", *Phys. Fluids*, 8, 2182-2189 (1965).

17. Reynolds, W.C., STANJAN, Stanford Univ. (1981).